Experimental and Theoretical Investigation of Decentralized Desalination System

اختبار عملي ونظري لنظام تحلية مياه لا مركزي

Mohamed Elsharkawy[a,1], Hossam AbdelMeguid[b,2], Ibrahim El-Sharkawy[b,3], and Lotfy Rabie[b]

[a]Taba desalination plant, Holding company of water and waste water north &south Sinai, Taba, Egypt.

[b]Mechanical Power Engineering Department, Faculty of Engineering, Mansoura University, El-Mansoura 35516, Egypt

[1] Email: moh.sharkawy8@gmail.com, Tel.: +201098816182
[2] Email: hssaleh@mans.edu.eg, Tel.: +201066464712
[3] Email:ielsharkawy@mans.edu.eg, Tel.: +201006107242

ملخص

لنقص الخبرة والمهارة الفنية الكافية فى المناطق النائية مع قلة التجمعات العمرانية ونُدرة موارد المياه العذبة تُعد وحدات تحلية المياه اللامركزية حل أمثل. وتمثل طريقة "الترطيب وإزالة الرطوبة" باستخدام مصادر حرارية منخفضة درجة الحرارة مثل الطاقة الشمسية أو الحرارة المفقودة فى العديد من العمليات المختلفة إحدى أهم التقنيات المستخدمة فى إنتاج المياه العذبة لامركزياً. وبناءاً عليه فقد تم عمل دراسة نظرية وعملية على هذه الطريقة. ففي هذا البحث تم عمل نموذج نظري لدراسة العوامل المختلفة التى تؤثر على الإنتاجية ولإثبات صحة هذا النموذج النظري تم عمل نموذج تجريبى لدراسة هذه العوامل عملياً. وتم تطوير برنامج حاسوب باستخدام الماتلاب (MATLAB) لحل النموذج النظري ومعالجة النتائج. برهنت النتائج العملية صحة النموذج النظرى حيث توافقت النتائج العملية والنظرية من حيث القيم المطلقة والمسار والاتجاه. وفُسر الفرق بين النتائج العملية والنظرية بالفروض المثالية لعمليات انتقال الحرارة والكتلة فى الاجزاء المختلفة أثناء عمل النموذج النظرى. وفى الدراسة العملية وجد أنه بزيادة معدل تصرف المياه الساخنة الداخلة إلى المرطب (المياه المغذية) تزداد الانتاجية حيث أن بزيادة معدل تصرف المياه المغذية من 0.05 كجم/ث إلى 0.08 كجم/ث تزداد الإنتاجية من 5.76 لتر/س إلى 8.04 لتر/س ومن 4.32 لتر/س إلى 5.76 لتر/س ومن 3.24 لتر/س إلى 4.08 لتر/س ومن 1.68 لتر/س إلى 2.16 لتر/س عند درجة حرارة المياه المغذية 70 و60 و50 و36 درجة مئوية على التوالى. كما أنه بزيادة معدل سريان الهواء من 0.055 كجم/ث إلى 0.1 كجم/ث تزداد الإنتاجية من 6.36 لتر/س إلى 7.32 لتر/س ومن 5.16 لتر/س إلى 5.64 لتر/س ومن 3.6 لتر/س إلى 4.08 لتر/س ومن 1.92 لتر/س إلى 2.22 لتر/س عند درجة حرارة المياه المغذية 70 و60 و50 و36 درجة مئوية على التوالى. بزيادة معدل تصرف مياه التبريد من 0.08 كجم/ث إلى 0.15 كجم/ث ومع ثبات المتغيرات الأخرى تزداد الانتاجية من 6.12 لتر/س إلى 6.84 لتر/س ومن 4.68 لتر/س إلى 5.28 لتر/س ومن 3.24 لتر/س إلى 3.84 لتر/س ومن 1.74 لتر/س إلى 2.04 لتر/س عند درجة حرارة المياه المغذية 70 و60 و50 و36 درجة مئوية على التوالى.

Abstract

This paper presents experimental and theoretical investigation of decentralized desalination system based on a humidification-dehumidification (HDH) process. HDH is one of the methods that employed in the decentralized systems in remote areas where there is lack of experienced operators, maintenance and water resources. HDH is suitable for remote areas that require small amount of fresh water. In the current work, a mathematical model is presented to investigate the effect of different operating parameters on the system productivity. A computer program based on MATLAB software is developed to solve the mathematical model and post-process the numerical results. In order to validate the mathematical model and verify the obtained numerical results, an experimental setup of decentralized HDH desalination system is designed and constructed. A series of experimental and numerical runs for different operating parameters are performed. The experimental data are compared with the numerical results and a good agreement in both values and trend is observed. The transient

Received: 31 March, 2014 - Revised: 9 June, 2014 - Accepted: 23 June, 2014

state behaviour of each component of the system and the influence of the different operating parameters on the system productivity are presented theoretically and experimentally.

Keywords: Desalination; Humidification; Dehumidification; Decentralized.

Nomenclature

A	heat transfer area [m^2]
As	surface area [m^2]
a	width [m]
β	temperature reciprocal [$℃^{-}$]
b	length [m]
Cp_w	specific heat of water [J/kg.K]
c	height [m]
Gr	Grashof number (The ratio of the buoyancy to viscous force)
g	gravitational acceleration [m/s^2]
h	convective heat transfer coefficient [$W/m^2.K$]
ha	enthalpy of air [J/kg]
k	thermal conductivity [W/m.K]
Lc	characteristic length [m]
loss	losses of component [Watt]
MCp	heat capacity [J/K]
ṁ	mass flow rate [kg/s]
Nu	Nusselt Number (convective heat transfer / Conductive heat transfer)
Pr	Prandtl number (Viscose diffusion rate / Surface diffusion rate) (Cp.μ/k)
p	perimeter [m]
Q	heater capacity [Watt]
Ra	Rayleigh number (Grashof number * Prandtl number) (Gr. Pr)
T	temperature [^oC]
Tf	average temperature [^oC]
U	Overall heat transfer coefficient [$W/m^2.K$]
w	specific humidity [kg_w/kg_a]
Z	insulation thickness [m]

Subscripts

a	air
amb	ambient
a1	air outlet from dehumidifier
a2	air inlet to humidifier
a3	air outlet from humidifier
cw	cooling water
DH	dehumidifier
H	humidifier
hor	horizontal
i	inlet
ins	insulation
Lc	characteristic length
loss	losses
mw	make up water
o	outlet
ost	outside storage tank
prod	product
st	storage tank
ver	vertical
w1	feed water inlet to humidifier
w2	water outlet from humidifier

1. Introduction

Interest in seawater desalination goes back to the fourth century BC, when Greek sailors used to obtain drinking water from seawater. The first work published on solar desalination was that of Arab alchemists in 1551 [1]. However, the first solar still was designed and constructed in Chile by the Swedish engineer, Carlos Wilson, in 1872 [1].

World-wide water scarcity, especially in the developing world, indicates a pressing need to develop inexpensive, decentralized small-scale desalination technologies which use renewable resources of energy.

Combining the principle of humidification–dehumidification (HDH) with solar desalination decreases the consumption of conventional energy resources in desalination plants and therefore appears to be the best method of water desalination in remote areas.

This section provides a comprehensive review of the state-of-the-art in one of the most promising of these technologies, HDH desalination technology.

A number of studies on solar desalination systems using HDH technique were presented in the literature [2-4]. Mostly, these studies include the performance evaluation of the HDH desalination systems under different systems operating parameters. In addition, in some of these studies, different types of solar collectors (water and air), humidifying towers and dehumidifying exchangers were designed and constructed, and their effects on the solar desalination system productivity were evaluated theoretically and experimentally [5-7]. Moreover, the influence of different system configurations, (such as with/without solar air and water heaters) on the solar desalination units productivity were investigated [8, 9]. As well, natural and forced air circulation solar HDH desalination were investigated [10]. In addition, a hybrid HDH-Flashing evaporating system and HDH-Compression systems were proposed and studied [11, 12].

During the last decade, a number of HDH desalination units were developed and tested [13, 14]. Dai and Zhang [15] studied experimentally a solar desalination system with HDH. The used process was based on the principle of open air-closed water cycles and forced air circulation. Mainly, a solar water heater, humidifier and condenser configure the system. The most important characteristic of the system is the ability to utilize efficiently low-grade heat resources, such as waste heat, geothermal, gas/oil/coal burning, etc. It was found that the performance of the system is strongly dependent on the rate of feed water temperature, the mass flow rate of salt water and the mass flow rate of the process air. In addition, it is reported that water productivity of the described solar desalination system is about 6.2 kg/m^2.day under optimal operating conditions.

Chafik [16] presented a seawater desalination process based on the stepwise heating-humidifying technique. The main feature of the suggested process is that the air is successively loaded with the water vapour up to relative high humidity, such as 10 or 15%. It was reported that, by this way, the airflow rate through the plant could be reduced and low investment and operating costs could be achieved. In addition, he developed two different types of the humidifier, which are pad humidifier and U-tube spray chamber humidifier. The experimental results of the humidifiers indicated that their efficiency is about 95%, and also, he tried to find out an optimum number of required heating/humidifying stages.

Amara et al. [17] carried out an experimental and theoretical study of a pad humidifier used in a multi-stage solar desalination process in Tunisia under different ambient and operating conditions. The mathematical formulation of the pad humidifier was developed and the non-linear system of equations was solved by using the numerical method, Newton-Raphson. The numerical results were compared to the experimental data to validate the numerical model and there was a good agreement between them.

Nafey et al. [18, 19] carried out a theoretical and experimental study of a HDH process using solar energy at the weather conditions of Suez City, Egypt. In the theoretical study, a mathematical model was developed, simulating the system, to study the effects of the different system configurations and operating conditions. The results showed that the productivity of the system increases with the increasing of air mass flow rate, solar air and water collector areas, and input solar energy. On the other hand, productivity of the unit decreases with the increasing of water mass flow rate. Finally, they reported that the wind speed and

ambient temperature have very small influence on the system performance.

This study aims to develop a mathematical model and validate it by using experimental data, and investigate theoretically and experimentally the effect of different operating parameters, such as mass flow rates of air and water and feed water temperature, on the productivity of a decentralized air HDH desalination system.

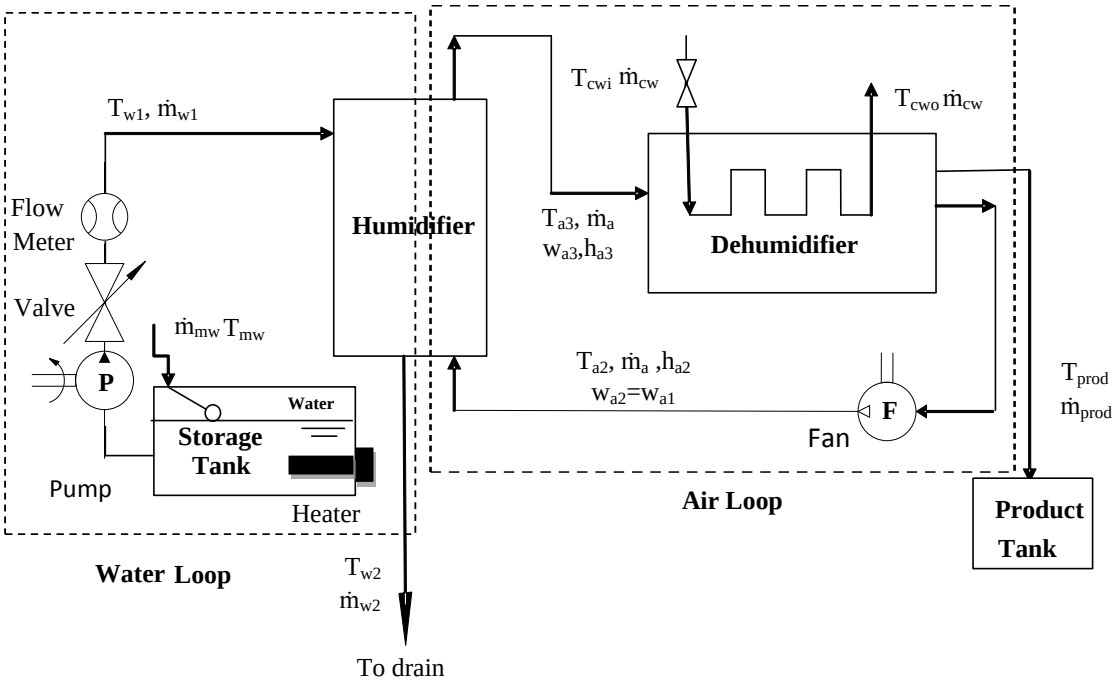

Figure 1 A schematic diagram of HDH desalination system.

2. Experimental set up

A schematic diagram of the HDH (Open water and closed air cycles) system is shown in Figure 1. The hot water is pumped (373 Watt centrifugal pump) from the storage tank and sprayed into the air humidifier. The air enters the humidifier from the bottom, where it contacts the falling hot water film at large mass transfer area of the packing. The remaining water is drained. The humid air passes through a dehumidifier (heat exchanger) for dehumidification (condensing air water contents) using cooling water, and then air is re-circulated to the humidifier again.

2.1 Humidifier

The humidifier unit contains five cassettes in series made of plastic material (polypropylene), which forms the wetted surface. The cross-sectional area of the cassette is 720 mm x 520 mm, and the thickness of each cassette is 170 mm. The packed pad has been mounted horizontally in a metal rack of dimensions: a_H= 530 mm width, b_H= 730 mm length and c_H= 1400 mm height. The rack has been made of galvanized steel of 1.5 mm thickness and has been insulated by foam of thickness 10 mm. Figure 2 shows a section view of the humidifier.

Figure 2 section view of the humidifier.

2.2 Dehumidifier

Air cooler heat exchanger of copper tubes, corrugated aluminium fins has been used as a dehumidifier. The total surface area of the dehumidifier is about 11 m^2. To prevent air leakage and heat gain, the dehumidifier heat exchanger has been packed by a metal case. The case has been constructed of 1.5 mm thick galvanized steel of dimensions a_{DH}= 400 mm width, b_{DH}= 950 mm length and c_{DH}= 330 mm height.

2.3 Water storage tank

The water storage tank has been constructed of 5 mm thick plastic tank of dimensions: 600 mm diameter, and 920 mm height. The tank is thermally insulated by glass wool of thickness 10 mm. It consists of one electric heater of capacity Q= 3 kW with a built-in thermostat. The heater was horizontally placed at the bottom of the tank. The heater was used to heat the water inside the tank to a certain temperature to investigate the effect of the feed water temperature on the system productivity. A constant temperature and head of water inside the storage tank during the experimental runs have been maintained.

3. Mathematical modelling

In order to apply the energy and mass balance equations for each of the system components, the following assumptions are applied to the present model:

1) Either laminar or turbulent flow is fully developed.
2) The effectiveness of the humidifying process is assumed to be unity, thus:
   a) The air leaving the humidifier is at saturation condition. Therefore, the wet-bulb and dry-bulb temperatures are identical.
   b) The temperature of water leaving the humidifier is equal to the wet-bulb temperature.
3) The dehumidification process lies on the saturation curve.
4) Temperature gradient inside the water storage tank is neglected (a perfect mixing is assumed).
5) The temperature of inlet water (feed water) is equal to the water temperature in the storage tank (no heat loss in the lines is assumed).
6) Cooling water temperature is constant during the day (infinite source of cooling is assumed).
7) Exit temperature of the condensate water and the outlet cooling water are equal to the dry-bulb temperature of the dehumidifier exit.

Applying the thermodynamic laws for the humidifier, dehumidifier, and storage tank as shown in Figure 1, the energy and mass balance equations can be written as:

3.1 Humidifier

Mass balance:

$$\dot{m}_{w1} + \dot{m}_a w_{a2} = \dot{m}_{w2} + \dot{m}_a w_{a3} \quad (1)$$

Heat balance:

$$MCp_H \frac{dT_H}{dt} = \dot{m}_{w1} Cp_w T_{w1} + \dot{m}_a h_{a2} - \dot{m}_{w2} Cp_w T_{w2} - \dot{m}_a h_{a3} - loss_H \quad (2)$$

$$MCp_H = MCp_{metal} + MCp_{packing} + MCp_{water} + MCp_{air} \quad (3)$$

The humidity and saturated air enthalpy are given by Al-Hallaj et al [20];

$$w_a = 2.19 * 10^{-6} T^3 - 1.85 * 10^{-4} T^2 + 7.06 * 10^{-3} T - 0.077 \quad (4)$$

$$h_a = 0.00585 T^3 - 0.497 T^2 + 19.87 T - 207.61 \quad (5)$$

3.2 Dehumidifier

Mass balance:

$$\dot{m}_{prod} = \dot{m}_a * (w_{a3} - w_{a1}) \quad (6)$$

Heat balance:

$$MCp_{DH}\frac{dT_{DH}}{dt} = \dot{m}_a h_{a3} + \dot{m}_{cw} Cp_w T_{cwi} - \dot{m}_a h_{a1} - \dot{m}_{cw} Cp_w T_{cwo} - \dot{m}_{prod} Cp_w T_{prod} - loss_{DH} \quad (7)$$

$$MCp_{DH} = MCp_{metal} + MCp_{cw} + MCp_{prod} + MCp_{air} \quad (8)$$

3.3 Water storage tank

Mass balance:

$$\dot{m}_{mw} = \dot{m}_{w1} - \dot{m}_{w2} \quad (9)$$

Heat balance:

$$MCp_{st}\frac{dT_{st}(t)}{dt} = Q_{heater} + \dot{m}_{w2} Cp_w T_{w2} + \dot{m}_{mw} Cp_w T_{mw} - \dot{m}_{w1} Cp_w T_{w1} - loss_{st} \quad (10)$$

$$MCp_{st} = MCp_{metal} + MCp_{water} \quad (11)$$

3.4 Heat losses from the system

- The heat lost from storage tank , [21]:

$$loss_{st} = A_{st} U_{loss} (T_{st} - T_{amb}) \quad (12)$$

$$U_{loss} = {}^{1}/_{(1/h_{o_{st}} + Z_{ins}/k_{ins})} \quad (13)$$

The relation between Nu and Ra for cylindrical shape, [22]:

$$Nu_{St} = \left\{ 0.6 + \frac{0.387 Ra_{Lc}^{\frac{1}{6}}}{\left[1 + (0.559/Pr)^{\frac{9}{16}}\right]^{\frac{8}{27}}} \right\}^2 \quad (14)$$

- The heat lost from the humidifier:

$$loss_H = 2h_{horH} a_H b_H (T_H - T_{amb}) + 2h_{verH} c_H b_H (T_H - T_{amb}) + 2h_{verH} c_H a_H (T_H - T_{amb}) \quad (15)$$

- The heat lost from the dehumidifier:

$$loss_{DH} = 2h_{horDH} a_{DH} b_{DH} (T_{DH} - T_{amb}) + 2h_{verDH} c_{DH} b_{DH} (T_{DH} - T_{amb}) + 2h_{verDH} c_{DH} a_{DH} (T_{DH} - T_{amb}) \quad (16)$$

The relation between Nu and Ra for horizontal plate, [22]:

$$Nu_{horH} = 0.27 Ra_{Lc}^{1/4} \quad (17)$$

For vertical plate, Churchill and Chu [22] proposed:

$$Nu_{verH} = \left\{ 0.825 + \frac{0.387 Ra_{Lc}^{1/6}}{\left[1 + (0.492/Pr)^{\frac{9}{16}}\right]^{8/27}} \right\}^2 \quad (18)$$

$$Ra_{Lc} = \frac{g\beta(T_H - T_{amb})Lc^3}{\nu^2} Pr \quad (19)$$

$$Lc = As/p \quad (20)$$

$$\beta = 1/T_f \quad (21)$$

$$T_f = \frac{T_H + T_{amb}}{2} \quad (22)$$

$$h = \frac{Nu * k}{Lc} \quad (23)$$

4. Numerical solution

A computer simulation program to solve the mathematical model of the system has been developed by means of MATLAB software to investigate the effect of the various operating parameters on the productivity of decentralized HDH desalination system. The transient state lumped parameter model has been solved numerically by employing the function ode45.

ode45 implements a version of the Runge-Kutta(RK) $4^{th}/5^{th}$ order algorithm [23]. That means the numerical solver ode45 combines a fourth-order method and a fifth-order method, both of which are similar to the classical fourth-order RK

method. The modified RK varies the step size, choosing the step size at each step in an attempt to achieve the desired accuracy. Therefore, the solver ode45 is suitable for a wide variety of initial value problems in practical applications.

5. Results and discussion

This section presents the experimental results, the validation of the developed mathematical model and a parametric study for the decentralized HDH desalination system. The parametric study of the developed mathematical model includes the effects of feed water mass flow rate and temperature, air mass flow rate, and cooling water mass flow rate on the system productivity.

5.1 Model validation

The numerical results and experimental data of the steady-state system productivity at different values of the feed water mass flow rate at temperatures of 36 °C and 50 °C are compared in Figure 3. It can be seen that the results obtained show a good agreement in both values and trend with relative error ranges from 3.9% to 6% for feed water temperature of 50 °C, and 6.8% to 12.1% for feed water temperature of 36 °C. This deviation can be attributed to the assumptions 3, 4, and 5 that assume ideal processes.

Figure 4 shows a comparison between the numerical results and experimental data of the steady-state system productivity at different values of the feed water mass flow rate at temperatures of 36 °C and 50 °C. There is a good agreement in both values and trend between the theoretical and experimental data. The deviation between the numerical results and the experimental data varies from 1.3% to 10.8% for feed water temperature of 50 °C, and from 6.3% to 9.2% for feed water temperature of 36 °C. These differences are due to the assumed perfect processes and ignoring the thermal and frictional losses in the system.

The numerical results and experimental data of steady-state productivity of the system at different values of the cooling water mass flow rate are compared in Figure 5. It can be seen from the figure that both results are matching with each other. Due to the assumed ideal processes and neglecting both frictional and thermal losses (assumptions 3, 6, and 7), a deviation of 3.6% to 7.1% for feed water temperature of 50 °C, and 6.8% to 8.1% for feed water temperature of 36 °C are observed.

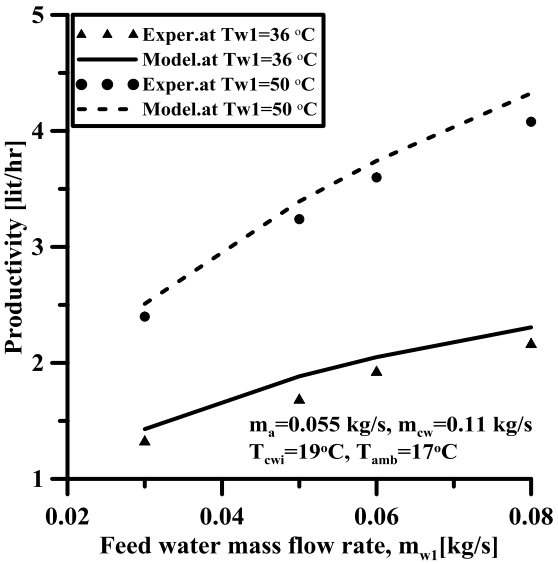

Figure 3 Comparison between experimental and numerical results of the steady-state production at different values of the feed water mass flow rate.

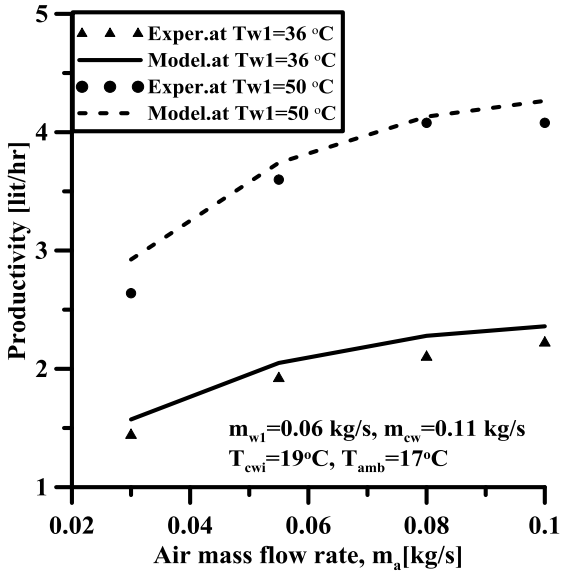

Figure 4 Comparison between experimental and numerical results of the steady-state production at different values of the air mass flow rate.

5.2 Experimental results

In order to measure the experimental data thermocouples connected to a temperature recorder have been used to measure the various temperatures, a water flow meter (rotameter) to measure the mass flow rate of water, and an anemometer is used to measure the mass flow rate of air.

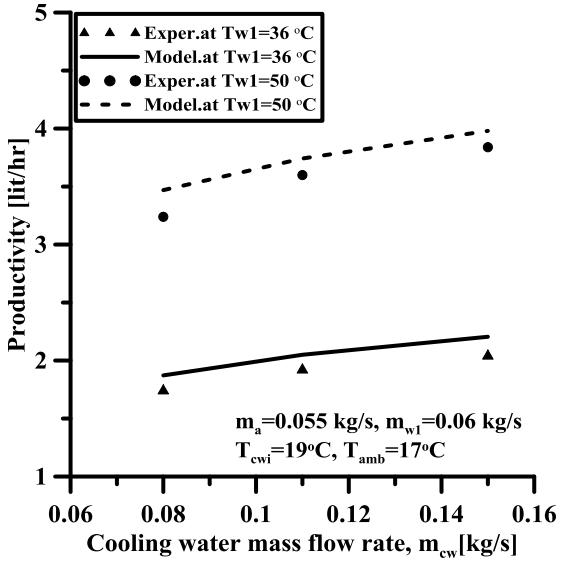

Figure 5 Comparison between experimental and numerical results of the steady-state production at different values of the cooling water mass flow rate.

The effect of feed water mass flow rate on the system productivity is presented in Figure 6. It depicts that the productivity of the system increases from 5.76 to 8.04 lit/hr and from 4.32 to 5.76 lit/hr for feed water temperature of 70 and 60°C, respectively. The results show that the productivity of the system increases with increasing the mass flow rate of feed water and the feed water temperature.

Increasing the water production with the feed water mass flow rate can be explained clearly with the aid of Figures 7 and 8. It can be seen that the difference between the outlet temperatures of the air leaving the humidifier, T_{a3}, and inlet temperatures, T_{a1}, increases as the feed water mass flow rate increases, thus relative humidity of the air increases. This is due to the increasing in contact surface area between the feed water and process air.

Figure 7 illustrates the transient variations of the humidifier inlet air temperatures, T_{a1}, at different feed water mass flow rates. For constant feed water temperature, the inlet air temperature increases gradually from the initial temperature of about 17°C (ambient temperature) to reach a steady-state operation in about 20 min. As well, it can be seen from the figure that as the feed water mass flow rate increases, the steady-state operation of the inlet air temperature increases.

Figure 8 depicts the transient trajectory of the humidifier outlet air temperatures, T_{a3}, at different feed water mass flow rates. The outlet air temperature rises from the initial temperature of about 17 °C to reach a steady-state operation in about 20 min for constant feed water temperature of 50 °C. In addition, the results showed that increasing the feed water mass flow rate increases the steady-state operation of the outlet air temperature.

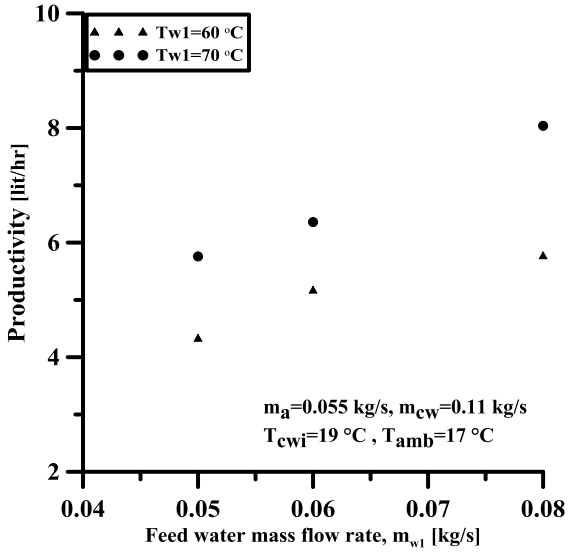

Figure 6 Effect of feed water mass flow rate on the system steady-state productivity.

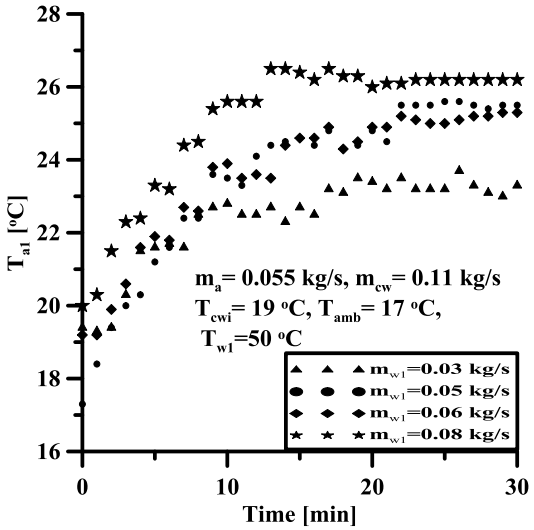

Figure 7 Transient variations of the inlet air temperatures, T_{a1}, at different feed water mass flow rates.

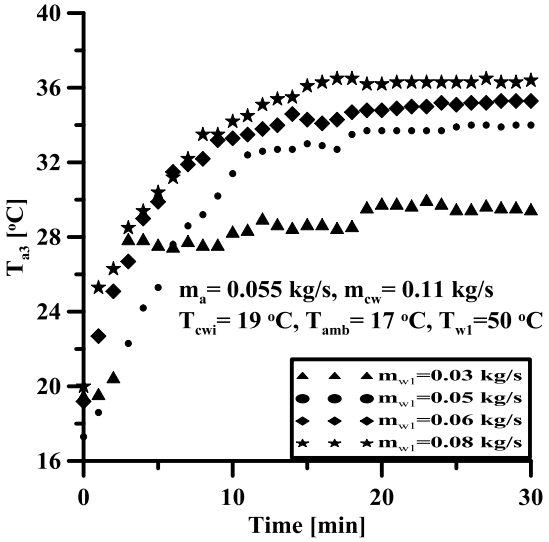

Figure 8 Transient variation of the outlet air temperature,T_{a3}, at different feed water mass flow rates.

5.3 Parametric study

A number of runs have been performed in order to assess the influence of the following operating parameters on the transient and steady-state productivity of the system:

- Mass flow rates of the feed water $\dot{m}_{w1}$;
- Mass flow rate of the process air $\dot{m}_a$;
- Mass flow rate of the cooling water $\dot{m}_{cw}$; and
- Feed water temperature.

Figure 9 depicts the transient variation of the system productivity at different values of feed water mass flow rate at constant feed water temperature of 50 °C. The system reaches a steady-state production after about 20 minutes due to thermal inertia of the system.

The effect of the feed water mass flow rate on the system steady-state productivity for air mass flow rate of 0.055 kg/s and cooling water of 0.11 kg/s at 19 °C is presented in Figure 10. It illustrates that the productivity of the system increases with increasing feed water mass flow rate. The theoretical results show that the decentralized HDH desalination system considered in this study produces 8.04

lit/hr in the steady-state operation at feed water temperature of 70 °C and mass flow rate of 0.08 kg/s.

Figure 11 shows the transient variation of the humidifier inlet air temperature, T_{a1}, with constant air mass flow rate at different feed water mass flow rates and constant inlet water temperature of 50 °C. The increase of feed water mass flow rate increases inlet air temperature. The steady-state operation is achieved after 20 min due to thermal inertia of the system.

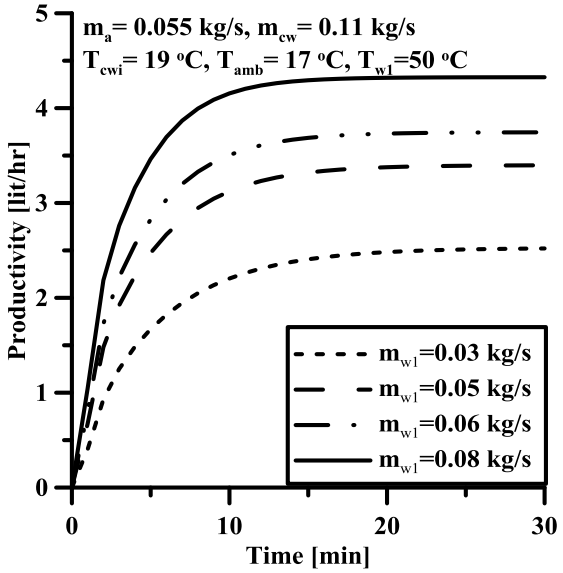

Figure 9 Transient production at different mass flow rates of feed water at a constant temperature of 50°C.

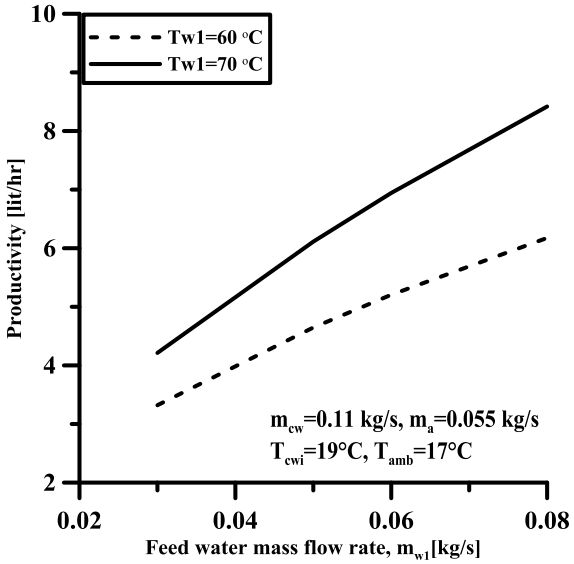

Figure 10 Effect of inlet hot water mass flow rate on productivity.

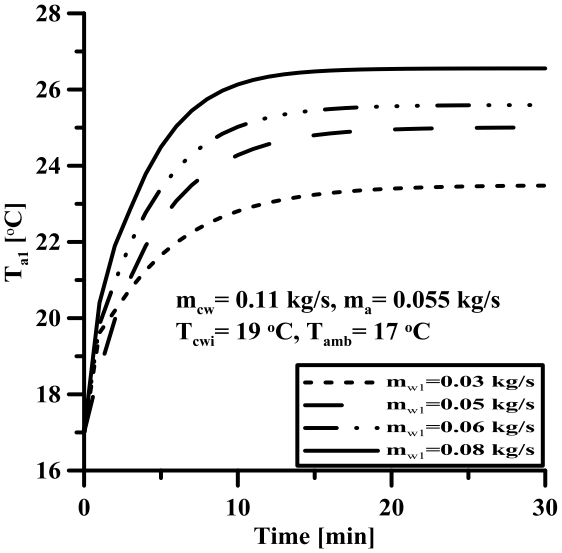

Figure 11 Inlet air temperatures, T_{a1}, of the humidifier at different feed water mass flow rates and inlet water temperature of 50°C.

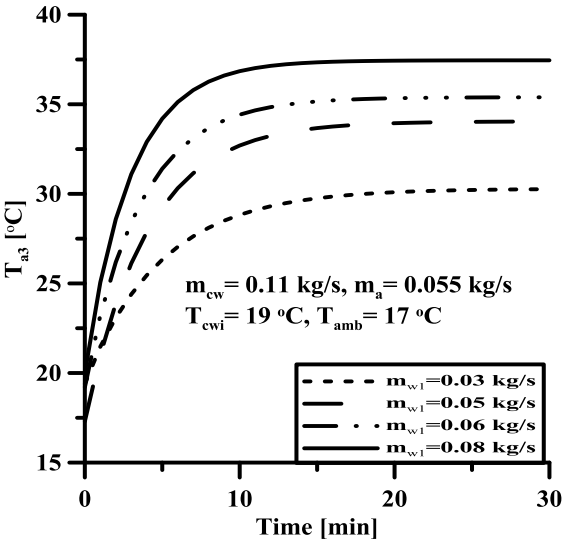

Figure 12 Outlet air temperatures, T_{a3}, of the humidifier at different feed water mass flow rates and inlet water temperature of 50 °C.

Figure 12 depicts the transient variation of the humidifier outlet air temperature, T_{a3}, with constant air mass flow rate at different feed water mass flow rates and constant inlet water temperature of 50 °C. The increase of feed water mass flow rate increases the wet-bulb temperature of the air leaving the humidifier and approaches to the inlet feed water temperature. Consequently, the moisture content of the air leaving the humidifier increases and a significant improvement on the system

productivity can be achieved by increasing the feed water mass flow rate.

Figure 13 illustrates the transient variation of the system productivity with different values of air mass flow rate at constant feed water flow rate of 0.06 kg/s, constant inlet water temperature of 50 °C, cooling water of constant mass flow rate of 0.11 kg/s, and constant inlet cooling water temperature of 19 °C. The system reaches the steady-state production after about 20 minutes due to thermal inertia of the system. The results also show that the system is capable of producing 4.26 lit/hr under the previously mentioned conditions and air mass flow rate of 0.1 kg/s.

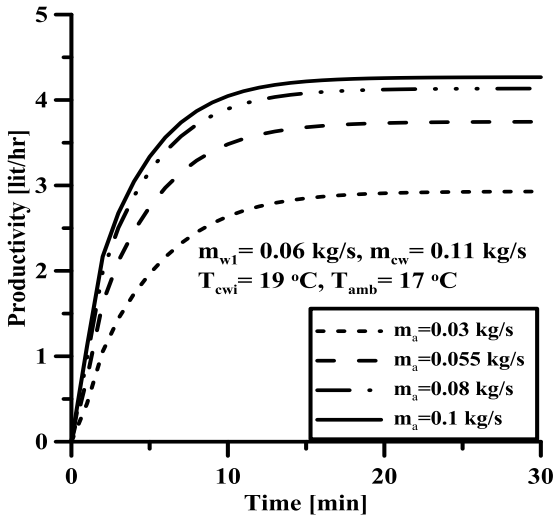

Figure 13 Transient production at different air mass flow rates and inlet water temperature of 50°C.

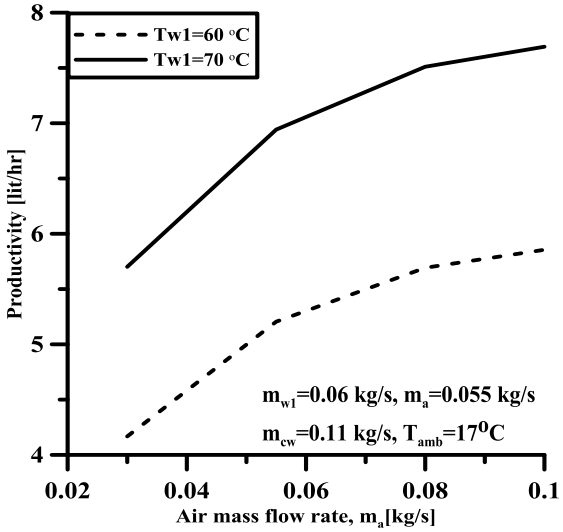

Figure 14 Effect of air mass flow rate on steady-state system productivity.

It can be observed from Figure 14 that the productivity of the system increases by increasing the air mass flow rate. This may be due to the fact that increasing the air mass flow rate increases the entrained water vapour and, therefore, increases the productivity. In addition, increasing the air mass flow rate increases the mass and heat transfer inside the humidifier, which increases the rate of vaporization of water and, hence, the productivity.

Figure 15 depicts the transient variation of the system productivity with different values of cooling water mass flow rate at constant feed water mass flow rate of 0.06 kg/s and inlet water temperature of 50°C.The system reaches the steady-state production after about 20 minutes due to thermal inertia of the system. The numerical results illustrate that the system could produce 3.98 lit/hr under the previously mentioned conditions and cooling water mass flow rate of 0.15 kg/s.

The results shown in Figure 16 illustrate the effect of cooling water mass flow rate on the steady-state system productivity. By increasing the cooling water mass flow rate, significant drop in the surface temperature of the cooler coil can be achieved and consequently, an increase of the rate of the condensation of the water content carried by the flowing air is achieved on the dehumidifier coil surface.

6. Conclusions

An experimental study was performed to investigate the effect of different operating conditions on the productivity of the desalination system using the humidification-dehumidification (HDH) process and to validate the developed mathematical model of the system.

The numerical results accord with the experimental data in values and trend with deviation ranges from 1.3% to 12.1% in the steady-state system productivity for different operating conditions.

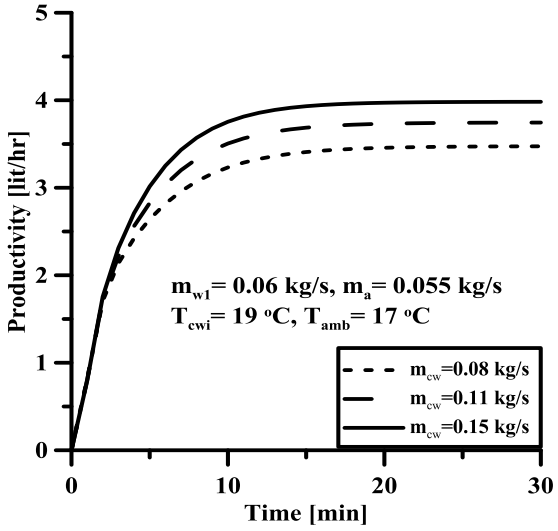

Figure 15Transient production at different mass flow rates of cooling water for a constant feed water mass flow rate of 0.06 kg/s and constant inlet water temperature of 50°C.

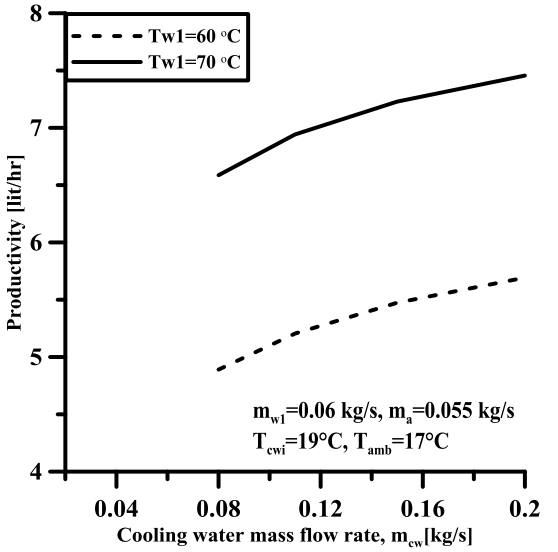

Figure 16 Effect of cooling water mass flow rate on the steady-state system productivity.

Both experimental data and numerical results show that the production increases by increasing feed water mass flow rate, air mass flow rate, cooling water mass flow rate, and feed water temperature.

For the considered system in the present study, the numerical results depict that the decentralized HDH desalination system with feed water mass flow rate of 0.08 kg/s at constant inlet water temperatures of 70 °C, 60 °C, 50 °C and 36 °C, is capable of producing steadily 8.42 lit/hr, 6.18 lit/hr, 4.32 lit/hr and 2.31 lit/hr, respectively. While the experimental data show that the system produces 8.04 lit/hr, 5.76 lit/hr, 4.08 lit/hr and 2.16 lit/hr for the same operating conditions.

Table 1 shows a comparison between this study and Kabeel et al [10].

Researcher name	Present study	Kabeel [10]
Max. Product [kg/h]	8.04	23
Feed water temperature, $T_{w1}[^0C]$	70	50:90
Feed water mass flow rate, $\dot{m}_{w1}$[kg/s]	0.08	0.01667 : 0.06667
Deviation between Exp & Theo	12.1% / 5.9 % (max /mean)	13% / 7-8% (max /mean)

Appendix

The values of constants used are;

Cpw=Cpwater=Cpcw=Cpprod=4.2kJ/kg.K

Cpair=Cpa= 1.007 kJ/kg.K

Cppacking= 1.9 kJ/kg.K

Cpmetal=0.42 kJ/kg.K for steel, 1.67 kJ/kg.K for plastic

The parameters measured while experimental runs;

T_{w1} (Feed water temperature)

$\dot{m}_{w1}$ (Feed water mass flow rate)

$\dot{m}_a$ (Air mass flow rate)

$\dot{m}_{cw}$ (Cooling water mass flow rate)

$\dot{m}_{prod}$ (Production mass flow rate)

T_{a3} (Outlet air temperature of humidifier)

T_{a1} (Inlet air temperature of humidifier)

T_{cwi} (Cooling water inlet temperature)

T_{cwo} (Cooling water outlet temperature)

T_{amb} (Ambient air temperature)

The parameters Computed while numerical runs;

All other parameters computed numerically while using the numerical model.

References

[1] G.D. Rai, Solar Energy Utilization: A Textbook for Engineering Students, Khanna Publishers, 1987.

[2] S. Al-Hallaj, S. Parekh, M.M. Farid, J.R. Selman, Solar desalination with humidification–dehumidification cycle: Review of economics, Desalination, 195(1–3) (2006) 169-186.

[3] J. Orfi, N. Galanis, M. Laplante, Air humidification–dehumidification for a water desalination system using solar energy, Desalination, 203(1–3) (2007) 471-481.

[4] C. Yamalı, İ. Solmus, A solar desalination system using humidification–dehumidification process: experimental study and comparison with the theoretical results, Desalination, 220(1–3) (2008) 538-551.

[5] A.M. Abdel Dayem, M. Fatouh, Experimental and numerical investigation of humidification/dehumidification solar water desalination systems, Desalination, 247(1–3) (2009) 594-609.

[6] G.P. Narayan, M.H. Sharqawy, E.K. Summers, J.H. Lienhard, S.M. Zubair, M.A. Antar, The potential of solar-driven humidification–dehumidification desalination for small-scale decentralized water production, Renewable and Sustainable Energy Reviews, 14(4) (2010) 1187-1201.

[7] D. La, Y. Dai, H. Li, Y. Li, J.K. Kiplagat, R. Wang, Experimental investigation and theoretical analysis of solar heating and humidification system with desiccant rotor, Energy and Buildings, 43(5) (2011) 1113-1122.

[8] E.K. Summers, M.A. Antar, J.H. Lienhard V, Design and optimization of an air heating solar collector with integrated phase change material energy storage for use in humidification–dehumidification desalination, Solar Energy, 86(11) (2012) 3417-3429.

[9] J.-h. Wang, N.-y. Gao, Y. Deng, Y.-l. Li, Solar power-driven humidification–dehumidification (HDH) process for desalination of brackish water, Desalination, 305(0) (2012) 17-23.

[10] A.E. Kabeel, M.H. Hamed, Z.M. Omara, S.W. Sharshir, Experimental study of a humidification-dehumidification solar technique by natural and forced air circulation, Energy, 68(0) (2014) 218-228.

[11] Y. Ghalavand, M.S. Hatamipour, A. Rahimi, Humidification compression desalination, Desalination, 341(0) (2014) 120-125.

[12] A.E. Kabeel, E.M.S. El-Said, A hybrid solar desalination system of air humidification, dehumidification and water flashing evaporation: Part II. Experimental investigation, Desalination, 341(0) (2014) 50-60.

[13] K. Bourouni, M.T. Chaibi, L. Tadrist, Water desalination by humidification and dehumidification of air: State of the art, Desalination, 137(1–3) (2001) 167-176.

[14] H. Müller-Holst, M. Engelhardt, W. Schölkopf, Small-scale thermal seawater desalination simulation and optimization of system design, Desalination, 122(2–3) (1999) 255-262.

[15] Y.J. Dai, H.F. Zhang, Experimental investigation of a solar desalination unit with humidification and dehumidification, Desalination, 130(2) (2000) 169-175.

[16] E. Chafik, A new seawater desalination process using solar energy, Desalination, 153(1–3) (2003) 25-37.

[17] M.B. Amara, I. Houcine, A. Guizani, M. Mâalej, Theoretical and experimental study of a pad humidifier used in a seawater desalination process, Desalination, 168(0) (2004) 1-12.

[18] A.S. Nafey, H.E.S. Fath, S.O. El-Helaby, A.M. Soliman, Solar desalination using humidification dehumidification processes. Part I. A numerical investigation, Energy Conversion and Management, 45(7–8) (2004) 1243-1261.

[19] A.S. Nafey, H.E.S. Fath, S.O. El-Helaby, A. Soliman, Solar desalination using humidification–dehumidification processes. Part II. An experimental investigation, Energy Conversion and Management, 45(7–8) (2004) 1263-1277.

[20] S. Al-Hallaj, M.M. Farid, A. Rahman Tamimi, Solar desalination with a humidification-dehumidification cycle: performance of the unit, Desalination, 120(3) (1998) 273-280.

[21] C. Yamalı, İ. Solmuş, Theoretical investigation of a humidification-dehumidification desalination system configured by a double-pass flat plate solar air heater, Desalination, 205(1–3) (2007) 163-177.

[22] S.W. Churchill, H.H.S. Chu, Correlating equations for laminar and turbulent free convection from a horizontal cylinder, International Journal of Heat and Mass Transfer, 18(9) (1975) 1049-1053.

[23] J.R. Dormand, P.J. Prince, A family of embedded Runge-Kutta formulae, Journal of Computational and Applied Mathematics, 6(1) (1980) 19-26.